

- TOLSTOV, G. P. (1976). *Fourier Series*. New York: Dover Publications.
- WILKINS, S. W. & STUART, D. (1986). *Acta Cryst.* **A42**, 197-202.
- WILKINS, S. W., VARGHESE, J. N. & LEHMANN, M. S. (1983). *Acta Cryst.* **A39**, 47-60, 594.
- WING, R. M., DREW, H., TAKANO, T., BROKA, C., TANAKA, S., ITAKURA, K. & DICKERSON, R. E. (1980). *Nature (London)*, **287**, 755-758.
- YU, F. T. S. (1976). *Optics and Information Theory*. New York: John Wiley.

*Acta Cryst.* (1989). **A45**, 10-20

## Infinite Periodic Minimal Surfaces and their Crystallography in the Hyperbolic Plane

BY J.-F. SADOE AND J. CHARVOLIN

*Laboratoire de Physique des Solides, Bâtiment 510, Université Paris-Sud, 91405 Orsay, France*

(Received 25 February 1988; accepted 4 July 1988)

### Abstract

Infinite periodic minimal surfaces are now being introduced to describe some complex structures with large cells, formed by inorganic and organic materials, which can be considered as crystals of surfaces or films. Among them are the spectacular cubic crystalline structures built by amphiphilic molecules in the presence of water. The crystallographic properties of these surfaces are studied from an intrinsic point of view, using operations of groups of symmetry defined by displacements on their surface. This approach takes advantage of the relation existing between these groups and those characterizing the tilings of the hyperbolic plane. First, the general bases of the particular crystallography of the hyperbolic plane are presented. Then the translation subgroups of the hyperbolic plane are determined in one particular case, that of the tiling involved in the problem of cubic structures of liquid crystals. Finally, it is shown that the infinite periodic minimal surfaces used to describe these structures can be obtained from the hyperbolic plane when some translations are forced to identity. This is indeed formally analogous to the simple process of transformation of a Euclidean plane into a cylinder, when a translation of the plane is forced to identity by rolling the plane onto itself. Thus, this approach transforms the 3D problem of infinite periodic minimal surfaces into a 2D problem and, although the latter is to be treated in a non-Euclidean space, provides a relatively simple formalism for the investigation of infinite periodic surfaces in general and the study of the geometrical transformations relating them.

### I. Introduction

Recent studies of some 3D crystalline structures with large cells have pointed out the limitation of the classical aspect of crystallography, as concerned with the study of periodic organizations of topologically

zero-dimensional objects such as atoms and molecules, and called for the introduction of more operative concepts, permitting analysis of them as periodic organizations of two-dimensional objects such as surfaces and films. Such structures are often observed in liquid crystals – the ‘bicontinuous’ cubic phases of lyotropics, the *D* phases and ‘blue’ phases of thermotropic smectics and cholesterics – but also in some biological and inorganic materials. The need for new terms to describe them was advocated in some recent papers (Scriven, 1976, 1977; Hyde & Andersson, 1984; Mackay, 1985; Mackay & Klinowski, 1986; Sadoc & Charvolin, 1986). Among these structures we are particularly interested in liquid crystalline ones, formed by amphiphilic molecules in the presence of water, which can be described as periodic entanglements of two fluids media separated by interfaces organized in a symmetric film exhibiting a very rich polymorphism (Luzzati, 1968; Ekwall, 1975). We have recently demonstrated that, in the case of the ‘bicontinuous’ cubic structures of these materials, the film built by the interfaces is supported by surfaces directly related to the *F*, *P* and *G* infinite periodic minimal surfaces (or IPMS) of the mathematicians (Charvolin & Sadoc, 1987). These surfaces can be described as periodic non-intersecting surfaces with zero mean curvature separating space in two identical labyrinths. Thus, the above structures are interesting not only on purely physicochemical grounds but, also, as actual structures modelling surfaces of great mathematical interest.

Our approach to the polymorphism of the structures formed by amphiphilic molecules is presented in Sadoc & Charvolin (1986), and its application to the case of ‘bicontinuous’ cubic structures is developed in Charvolin & Sadoc (1987). It is based upon the idea that a geometrical frustration, related to local interactions of the molecules and packing constraints, takes place within the film. This frustration is relaxed if the film is transferred into the 3D space with positive

Gaussian curvature  $S_3$ , or the hypersphere. Therein, the film built by the interfaces is supported by the spherical torus  $T_2$ , a surface of genus 1 without curvature separating  $S_3$  into two identical subspaces. Then, in order to come back to the Euclidean space  $R_3$  in which the actual structures are embedded, the curvature of the curved space  $S_3$  is suppressed by the introduction of Volterra defects of rotation, or disclinations, around the symmetry axes of the relaxed structure in  $S_3$ . The main consequence of this procedure is that the spherical torus of genus 1, which admits a  $\{4, 4\}$  tiling, is transformed into IPMS of negative curvature admitting a  $\{6, 4\}$  tiling. It is therefore tempting to associate these IPMS to a particular surface of constant negative Gaussian curvature, the hyperbolic plane admitting a  $\{6, 4\}$  tiling, as they have the same local properties. However, it is known that the hyperbolic plane cannot be embedded in  $R_3$ , while the surfaces obtained by the mapping of  $S_3$  into  $R_3$  must be. This means that these surfaces cannot be confused with the whole hyperbolic plane. Nevertheless, there are strong relationships between them, and it is the purpose of this article to bring them out. In order to make the nature of the relationships between the hyperbolic plane and the IPMS manifest, we can use a simple but useful analogy between the hyperbolic plane and the Euclidean plane, which shall be used at other places in the text for other illustrative analogies. The relationships existing between the hyperbolic plane and the IPMS are indeed of the same nature as those existing between the Euclidean plane and other surfaces without Gaussian curvature, such as a cylinder or a torus. A cylinder is obtained by cutting a strip from a plane and identifying the two boundaries, a torus of genus 1 is obtained by cutting a square, or a rectangle, in a plane and identifying the opposite edges 2 by 2. If a Cartesian  $\{4, 4\}$  net of unit cells is defined on the original plane, the identifications needed for building the cylinder and the torus are identical to the writing of Born-von Karman conditions preserving the translational periodicity of the plane. Thus, new surfaces can be built from the plane by substituting some operations of translation by identifications. We show in this paper that similar substitutions in the translation subgroups of the hyperbolic plane lead to the building of surfaces with negative Gaussian curvatures embedded in  $R_3$ , which are the classical IPMS.

## II. Symmetry groups in the hyperbolic plane

### II.1. Generalities on symmetry groups

Symmetries and their groups are described in classical books (Coxeter & Moser, 1957; Magnus, 1974; Hilbert & Cohn-Vossen, 1983) and particular properties of the hyperbolic plane, useful in statistical mechanics, have been recently presented by Balzacs

& Voros (1986). We therefore give here just the main tools needed for our approach and refer the reader to these sources for further details.

We make use of Poincaré's representation of the hyperbolic plane (Hilbert & Cohn-Vossen, 1983; Coxeter, 1961). In this representation the whole hyperbolic plane is contained within a disk, the limiting circle of this disk represents the points at infinity of the plane and the family of circles orthogonal to this limit represents the geodesic lines. A mirror operation in the hyperbolic plane is represented by an inversion operation in a 'geodesic' circle and a direct displacement is the product of two such mirror operations, quite similarly to what happens in the Euclidean plane where rotation or translation are products of two mirror operations in two intersecting or parallel straight lines. However, because of the particular geometry of the hyperbolic plane, where one line can have two parallels passing through one point and non-intersecting lines are not necessarily parallels, as shown in Fig. 1(a), there are three types of direct displacements in this plane, as shown in Fig. 1(b). They are: rotations, obtained by products of mirror operations in two intersecting 'geodesic' circles, not on the limit circle; translations, obtained by products of mirror operations in two non-intersecting 'geodesic' circles; and parabolic displacements, obtained by products of mirror operations in two parallel 'geodesic' circles, *i.e.* having a common point at 'infinity' on the limiting circle.

Among all the symmetry groups of the hyperbolic plane, we shall consider discrete groups associated with the  $\{6, 4\}$  tiling only. As said before, this tiling is imposed by the disclination process needed to map  $S_3$  onto  $R_3$  and transforming the spherical torus into a surface with negative Gaussian curvature (Sadoc & Charvolin, 1986; Charvolin & Sadoc, 1987).

### II.2. Symmetry groups of the $\{6, 4\}$ tiling

Regular tilings of surfaces with constant curvature are built by reflections in three mirrors defined by the three sides of a rectangular triangle of geodesics, called an orthoscheme triangle or asymmetric unit

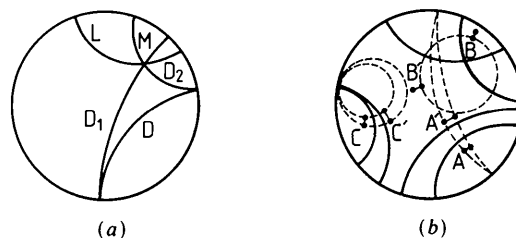


Fig. 1. Geometry of the hyperbolic plane: (a) parallel lines  $D_1$  and  $D_2$  to line  $D$  and (b) direct displacements, translation  $A-A'$ , rotation  $B-B'$  and parallel displacement  $C-C'$ . Dashed circles are the trajectories of points. Thick circles are mirrors.

(Coxeter, 1961), as shown in Fig. 2. The set of replicas of one orthoscheme obtained by the repetitions of these reflections covers the surface totally, without overlap. For instance, in the Euclidean plane, the  $\{6, 3\}$  and  $\{3, 6\}$  regular tilings of hexagons and triangles are obtained from an orthoscheme with angles  $\pi/2$ ,  $\pi/6$ ,  $\pi/3$ , and the  $\{4, 4\}$  regular tiling of squares is obtained from an orthoscheme with angles  $\pi/2$ ,  $\pi/4$ ,  $\pi/4$ . Similarly, on the sphere, each of the Platonic spherical polyhedra can be obtained from its own orthoschemes; the examples of the dodecahedron and the icosahedron obtained from the non-Euclidean orthoscheme with angles  $\pi/2$ ,  $\pi/3$ ,  $\pi/5$  are given in Fig. 3. The orthoscheme triangle is the fundamental region of the symmetry group; two points of the same fundamental region are not related by a symmetry operation and all points related by a symmetry operation are equivalent to one point of the orthoscheme.

The  $\{6, 4\}$  tiling of the hyperbolic plane is obtained from a non-Euclidean orthoscheme with angles  $\pi/2$ ,  $\pi/4$ ,  $\pi/6$ , as shown in Fig. 4. The sum of these angles is smaller than  $\pi$ , because of the negative Gaussian curvature of the hyperbolic plane, and the area  $S$  of the orthoscheme is given by Gauss's relation  $S = [\pi - (\pi/2 + \pi/4 + \pi/6)]/K$ , where  $K$  is the Gaussian curvature (Hilbert & Cohn-Vossen, 1983; Coxeter, 1961). Notice that the hexagonal element of the  $\{6, 4\}$  tiling is obtained by reflections in the mirrors defined by the sides of the angle of  $\pi/6$ ; reflections in the mirrors defined by the sides of the angle of  $\pi/4$  would

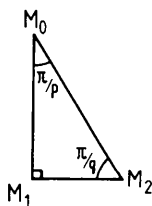


Fig. 2. The orthoscheme triangle  $M_0M_1M_2$  defining a  $(p, q)$  tiling.

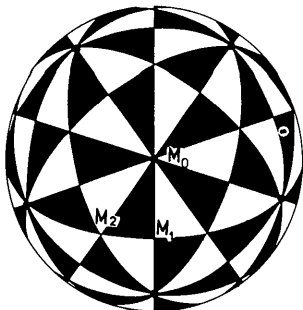


Fig. 3. Tiling of a sphere with an orthoscheme triangle having angles  $\pi/2$ ,  $\pi/3$  and  $\pi/5$ . The dodecahedral and icosahedral tilings obtained from it can be easily recognized.

give the square element of the  $\{4, 6\}$  tiling which is the dual of  $\{6, 4\}$  and has the same symmetry group.

Following Coxeter & Moser (1957) we denote by  $[6, 4]$  the symmetry group of this tiling. This group is defined by three generators  $R_1, R_2, R_3$ , which are the reflections in the orthoscheme sides, and the six relations

$$R_1^2 = R_2^2 = R_3^2 = (R_1R_2)^6 = (R_2R_3)^4 = (R_1R_3)^2 = I.$$

Among all the symmetry operations obtained by combining these generators several times and in different orders, as the reflections do not commute, several are translations. We now focus on the translation subgroup of the  $[6, 4]$  symmetry group. The approach is closely similar to that used in the crystallography of 2D structures. It consists of identifying a translation subgroup, called the lattice, defined by its fundamental region, called the unit cell.

### II.3. Generalities on translation subgroups

It is possible to find such a subgroup by considering that its unit cell can be a polygon with a number of sides divisible by four, except four itself which leads to translations in the Euclidean plane. The sum of the angles of this polygonal cell must be  $2\pi$  and each side must be associated with a non-adjacent side of the same length by a translation (Hilbert & Cohn-Vossen, 1983, p. 259). If there are  $4g$  sides, there are  $2g$  such translations ( $A_1, A_2, A_3, \dots, A_{2g}$ ) and their inverse. These  $2g$  translations are generators, whose combinations constitute the translation subgroup. This is a non-Abelian group as translations in the hyperbolic plane do not commute. The generators are related by

$$A_1A_2A_3, \dots, A_{2g}A_1^{-1}A_2^{-1}A_3^{-1}, \dots, A_{2g}^{-1} = I.$$

Notice that the relation depends on the way the sides of the polygonal cells are associated. The relation given above corresponds to the pairing of the sides shown in Fig. 5, but other pairings may be chosen (Magnus, 1974; Hilbert & Cohn-Vossen, 1983). Notice also that when  $g = 1$ , in the Euclidean plane,

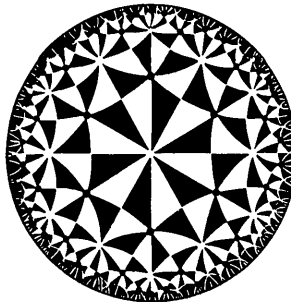


Fig. 4. Tiling of a hyperbolic plane with an orthoscheme triangle having angles  $\pi/2$ ,  $\pi/4$  and  $\pi/6$ . The  $\{6, 4\}$ ,  $\{4, 6\}$  and  $\{6, 6\}$  tilings obtained from it can be easily recognized.

the relation becomes  $A_1 A_2 A_1^{-1} A_2^{-1} = I$  and shows that translations commute in this case.

In 2D crystallography there are two ways of looking at the unit cell. For instance, with the square lattice of the Euclidean plane, the square cell can be looked at either as the fundamental region of the infinite plane or as the surface of the torus obtained by identifying its opposite sides and its vertices all together. The second point of view corresponds to the writing of the Born-von Karman conditions of periodicity and, in this case, all points equivalent in a translation are identified. These two points of view are equally valid in the hyperbolic case. The 4g-gon can be looked at either as a fundamental region for the translation subgroup or as a toroidal surface obtained by identifying its sides two by two and its vertices all together. This allows the use of classical topological theorems to characterize the unit cell. Euler's relation shows that its genus is  $g$ , when considered as a torus, and Gauss-Bonnet's theorem shows that its area is  $S = 4\pi(g-1)/K$ , where  $K$  is the Gaussian curvature of the hyperbolic plane (Hilbert & Cohn-Vossen, 1983).

#### II.4. Translation subgroups of the $[6, 4]$ group

The very nature of IPMS provides a clue to determine the lowest genus possible for their unit cell and, therefore, the essential features of the polygonal unit cell in the hyperbolic plane as discussed above. The surface enclosed in the primitive unit cell of an IPMS is a 3D fundamental region. If the opposite faces of this cell are identified two by two, a toroidal surface is obtained, embedded in a space which is the hypertorus  $T_3$ . This surface has a particular genus  $g$ , which is defined as that of the IPMS, and this genus must also be that of the toroidal surface built from the unit cell in the hyperbolic plane. This genus cannot be smaller than 3, as the identification of the six faces of the 3D cell leads to the formation of a toroidal surface having at least three handles. The genus could be larger than 3 but, as the IPMS studied up to now are of genus 3, we shall restrict our developments to this value of  $g$ .

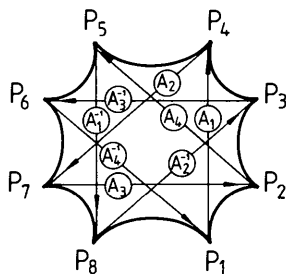


Fig. 5. A fundamental region for a translation in a hyperbolic plane and the pairing of its sides.

Thus the smallest translation cell in the hyperbolic plane associated with IPMS of genus 3 is a dodecagon of area  $8\pi/K$  and, as the orthoscheme triangle of the  $\{6, 4\}$  tiling has an area of  $\pi/(12K)$ , this translation cell contains 96 orthoschemes. A drawing of the dodecagonal fundamental region in the Poincaré representation is given in Fig. 6. All its angles are equal to  $\pi/6$  and the lengths of its sides are alternately equal to the double side and the double diagonal of a square of the  $\{4, 6\}$  tiling. There are different ways to associate the sides of the dodecagon two by two which result in different subgroups of translation in  $[6, 4]$ . Among all these possibilities we choose that which corresponds to the normal subgroup, *i.e.* the subgroup which is globally invariant in transformations of its elements by elements of the group  $[6, 4]$ .

We call  $t_1, t_2$  and  $t_3$  the translations relating large opposite sides, and  $\tau_1, \tau_2$  and  $\tau_3$  the translations relating small opposite sides. If we label the angles of the dodecagon from 1 to 12, all angles reproduced by these translations around one vertex of the original dodecagon appear in the order 1, 6, 11, 4, 9, 2, 7, 12, 5, 10, 3 and 8. This is also the order of the vertices of a star polygon  $\{12/5\}$ . The translations  $t_i$  and  $\tau_i$  are the generators of the translation subgroup with the relation

$$t_3^{-1} \tau_2^{-1} t_1^{-1} \tau_3^{-1} t_2^{-1} \tau_1^{-1} t_3 \tau_2 t_1 \tau_3 t_2 \tau_1 = I,$$

as can be seen by following the successive images of vertex 1 on the dodecagon. We call this normal subgroup  $\Phi_3^N$ . In Appendix A we show that  $t_i$  and  $\tau_i$  are elements of  $[6, 4]$  and  $[6, 6]$ . As already said, there are other translations in the  $[6, 4]$  group associating two non-opposite sides of the dodecagonal cell, as found in Hilbert & Cohn-Vossen (1983), which are elements of another subgroup of translation, isomorphic to  $\Phi_3^N$ , but not normal.

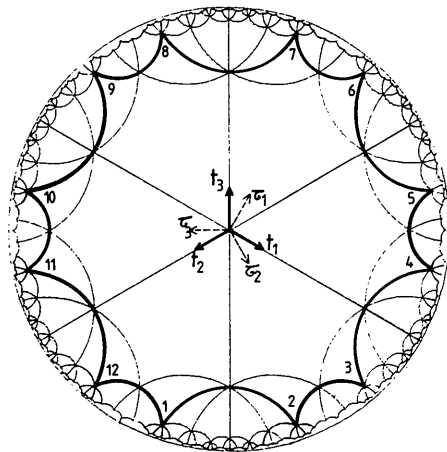


Fig. 6. The dodecagonal fundamental region for a subgroup of translation in the  $\{6, 4\}$  tiling of a hyperbolic plane and the six generators  $t_i$  and  $\tau_i$ . Sides 1-2 and 8-7 are equivalent by translation  $t_3$ , sides 5-4 and 10-11 are equivalent by translation  $\tau_3$ .

Among the translations defined by the generators  $t_i$  and  $\tau_i$  those associated with Petrie's polygons of the  $\{6, 4\}$  tiling are particularly important in our problem. A Petrie polygon is drawn along the sides of the tiling in such a way that two consecutive sides, but not more, belong to a given tile of the tiling. An important property of a Petrie polygon of a tiling  $\{p, q\}$  is that it is invariant by the product  $R_1 R_2 R_3$ , where  $R_1, R_2, R_3$  are the reflections in the sides of the orthoscheme triangle of the tiling (Coxeter & Moser, 1957, p. 54). This operation is a glide reflection and its square is a pure translation. Thus, a Petrie polygon defines a translation. Petrie polygons of the  $\{6, 4\}$  and  $\{4, 6\}$  tilings are drawn in Fig. 7, together with the geodesic line of the hyperbolic plane globally invariant in this translation and which contains the common points of the two Petrie polygons. Both polygons define the same translation. Another translation of the same type can also be defined considering the  $\{6, 6\}$  tiling of the same hyperbolic plane. This tiling is a subgroup of  $\{6, 4\}$  as its orthoscheme triangle with angles  $\pi/2, \pi/6$  and  $\pi/6$  is made with two juxtaposed orthoschemes of  $\{6, 4\}$ . The Petrie polygon of  $\{6, 6\}$  and its translation, which is also an element of  $\{6, 4\}$ , are drawn in Fig. 8.

We call these two translations  $P_{64i}$  and  $P_{66i}$ , referring to the type of Petrie polygon used to define them, and we now determine their expressions in terms of the generators  $t_i$  and  $\tau_i$ . For this, we choose a particular system of mirrors permitting the construction of translations  $t_i, \tau_i, P_{64i}$  and  $P_{66i}$ . These mirrors are the sides of one hexagon of the  $\{6, 4\}$  tiling and the symmetry axes normal to these sides; they are labelled as  $A_i, B_i$  and  $M_i$  in Fig. 9. Then, if one considers that the operations act from left to right,

$$\begin{aligned} t_i &= A_i B_i, & \tau_k &= B_j A_i B_i A_j, \\ P_{64i} &= M_k B_k M_j A_j, & P_{64i} &= M_k A_k M_j B_j, \\ P_{66i} &= A_j A_k, & P_{66i} &= B_j B_k, \\ P_{64i}^3 &= \tau_j^{-1} t_i \tau_k & \text{and} & \quad P_{66i}^2 = t_i \tau_i^{-1} t_k^{-1}. \end{aligned}$$

$P_{64i}$  and  $P_{66i}$  cannot be expressed in terms of  $t_i$  and  $\tau_i$ , and are therefore not elements of  $\Phi_3^N$ , but  $P_{64i}^3$  and  $P_{66i}^2$  are.

### III. Three IPMS of genus 3 and the hyperbolic plane

These three surfaces are the so-called  $P$  and  $F$  surfaces of Schwarz (1890) and the gyroid  $G$  of Schoen (1970). They can be defined in the Euclidean space  $R_3$  as periodic non-intersecting surfaces of zero mean curvature, separating  $R_3$  into two congruent ( $P$  and  $F$ ) or oppositely congruent ( $G$ ) labyrinths of different connectivities which are described in Appendix B. The surfaces are all built from orthoscheme triangles with angles  $\pi/2, \pi/4$  and  $\pi/6$  (Schwarz, 1890; Schoen, 1970; Hyde & Andersson, 1984; Mackay,

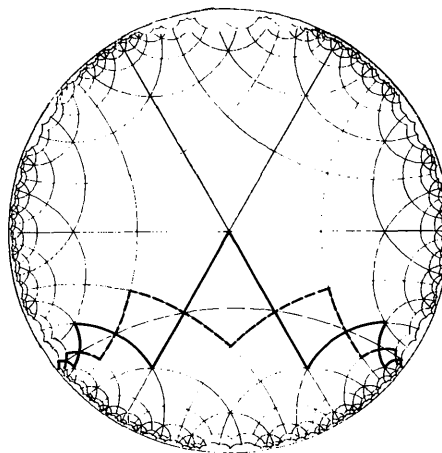


Fig. 7. Petrie polygons for the  $\{6, 4\}$  and  $\{4, 6\}$  tilings and the geodesic line invariant by translation.

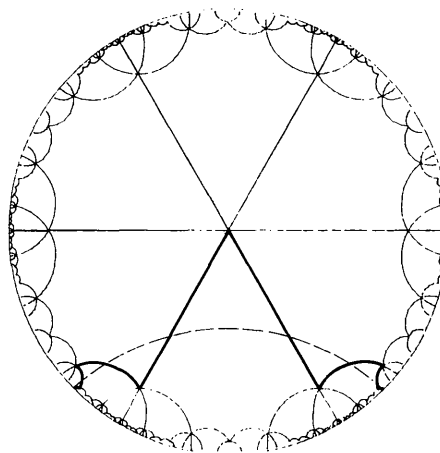


Fig. 8. Petrie polygon for the  $\{6, 6\}$  tiling and the geodesic line invariant by translation.

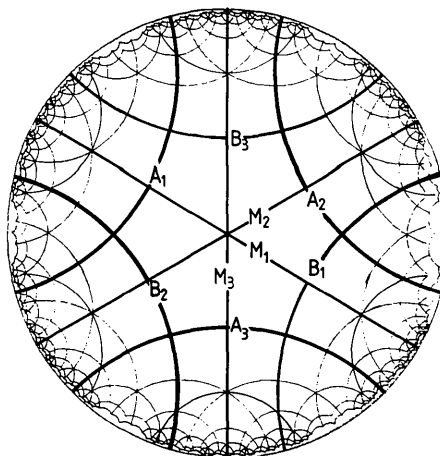


Fig. 9. Mirrors used to define the elementary translations.

1985; Mackay & Klinowski, 1986; Charvolin & Sadoc, 1987) and can therefore be described by the  $[6, 4]$  symmetry group of the hyperbolic plane studied above; although they issue from the same hyperbolic plane, they are distinct in  $R_3$  because the orthoscheme triangles have differently curved sides (Charvolin & Sadoc, 1987).

III.1. Schwarz's  $P$  surface

This is the simplest of the three surfaces. It separates two congruent labyrinths of connectivity 6, formed by the edges of simple cubic lattices, the vertices of one labyrinth being at the centres of the cubes of the other. Topological analogues of surface  $P$  are represented in Fig. 10. They are infinite periodic polyhedra built with either square or hexagonal flat faces, meeting 6 by 6 or 4 by 4 at every vertex respectively. They are obviously tilings of the  $\{4, 6\}$  or  $\{6, 4\}$  types and are therefore called  $\{4, 6\}$ - $6t$  or  $\{6, 4\}$ - $6t$ , where  $6t$  is the number of tunnels formed by the surface (Wells, 1977; Coxeter, 1968). These topological analogues are quite useful to relate the  $P$  surface to the  $\{6, 4\}$  tiling of the hyperbolic plane. For this it is advisable to choose the centre of the cubic cell on the surface itself and not at a vertex of the labyrinth, as is usually done (Charvolin & Sadoc, 1987). The best choice is the centre of a hexagon in the  $\{6, 4\}$ - $6t$  case, or the vertex of a square in the  $\{4, 6\}$ - $6t$  case, as shown in Fig. 11. With this choice the part of the polyhedron enclosed in the unit cell is similar to the dodecagonal fundamental region of the  $\Phi_3^N$  subgroup. It is a dodecahedron with non-equal sides, the short and long sides being equal to two sides and two diagonals of a square respectively. It appears also that the vertices of this dodecahedron are joined two by two, following the rule shown in Fig. 11 where they have been numbered as in Fig. 6; for instance, vertices 1 and 10 are identified together. These identifications correspond to the building of the tunnels formed by four squares.

This identification procedure is strictly analogous to the one which is used when a cylinder is built by wrapping of a plane, as shown in Fig. 12. The  $\{4, 4\}$  tiling of the plane defines a translation subgroup with generators  $a_1$  and  $a_2$  and the cylinder has the same

group but with the identification rule  $a_1^4 = I$ . Thus if we return to our problem, it is clear from Figs. 8 and 11 that the unit cell of the  $P$  surface is obtained from the hyperbolic tiling if the identification rule  $P_{66i}^2 = I$  is adopted. On the hyperbolic tiling all vertices of dodecagons are equivalent by the translations of the subgroup  $\Phi_3^N$ . On the  $P$  surface all points obtained from one point by the operation  $P_{66i}^2$  are identified in one single point. The symmetry operations on the  $P$  surface, an intrinsic point of view, are elements of the subgroup  $\Phi_3^N$  in which all elements  $P_{66i}^2$ , and elements obtained by transforming  $P_{66i}^2$  by other elements of  $\Phi_3^N$ , are forced to be identity operations. Some parts of the hyperbolic plane must be cut out to make the identifications leading to the  $P$  surface possible. These are shown in Fig. 13, in the case of the  $\{4, 6\}$  tiling corresponding to the  $\{4, 6\}$ - $6t$  structure of Fig. 11.

A consequence of this is that the generators  $t_i$  and  $\tau_i$  commute and that all translations have the form  $t_1^u t_2^v t_3^w$ ,  $\tau_i$  being expressed in terms of  $t_i$ . This results from  $P_{66i}^2 = t_j \tau_i^{-1} t_k^{-1} = I$  which leads to  $\tau_i = t_k^{-1} t_j$ . The commutation is demonstrated in Appendix C for the three examples. The commutativity and the expression of all translations in terms of three generators prove that the subgroup of translations obtained from  $\Phi_3^N$ , including the identifications, is isomorphic to the subgroup of translations in a

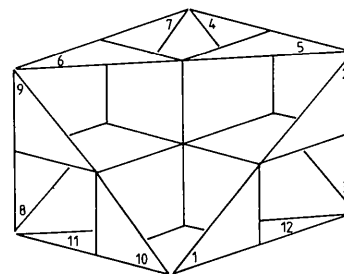


Fig. 11. The identification of the vertices of the dodecagonal cell for the polyhedron of Fig. 10(a), leading to an element of surface topologically equivalent to that of the cell of the  $P$  surface. This dodecagonal cell is contained in a cube. The polyhedron of Fig. 10(a) is obtained by reproducing this cube with the translation operations defined by its edges. For instance the juxtaposition of the two triangles containing numbers 10 and 3 builds a square of this polyhedron.

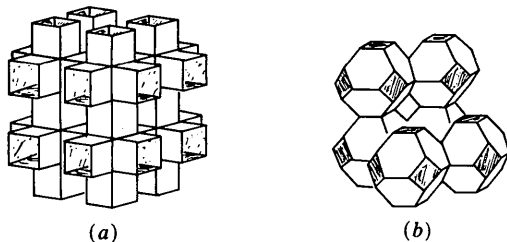


Fig. 10. Two infinite polyhedra topologically equivalent to the  $P$  surface. (a)  $\{4, 6\}$ - $6t$  and (b)  $\{6, 4\}$ - $6t$ .

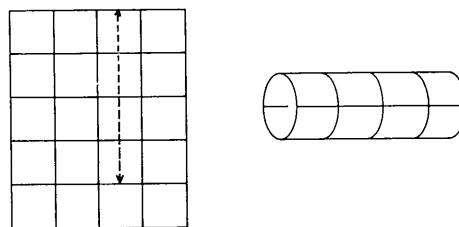


Fig. 12. The plane with a square tiling and the cylinder obtained from it by the identification  $a_1^4 = I$ .

Euclidean 3D lattice. In this intrinsic point of view the translations are displacements along geodesic lines on the surface, but two equivalent points are also equivalent by a translation in the Euclidean space in which the surface is embedded. The  $P$  surface is also a crystal in the Euclidean 3D space.

### III.2. Schwarz's $F$ surface

This surface separates two congruent labyrinths of connectivity 4 whose axes are parallel to the directions of the diagonals of a simple cubic packing. A topological analogue of this surface is represented in Fig. 14. It is a periodic infinite polyhedron built with flat hexagonal faces meeting 6 by 6 at every vertex. The primitive unit cell of this polyhedron is a rhombohedron and, if we put its centre at the centre of a hexagonal face, the part of polyhedron enclosed in this cell is the folded dodecagon shown in Fig. 15. We find here again a dodecagonal fundamental region, as in the case of the  $P$  surface, and we shall find one for the  $G$  surface also. We recall that this is quite normal as we consider surfaces of genus 3 obtained from the same hyperbolic plane with a  $\{6, 4\}$  tiling. The difference between the  $P$  and  $F$  surfaces appears immediately if one considers the vertices which are identified. For instance, if the vertices of

the dodecagon are numbered as in Fig. 6, vertex 1 is now identified with vertex 4 and not with vertex 10, as it was in the case of the  $P$  surface. Thus, these surfaces are built from the same fundamental region of the hyperbolic plane, and therefore have the same intrinsic curvature, but differ in the ways the identifications are made. This makes apparent what is implied when one of these surface is transformed into another by Bonnet's transformation (Hyde & Andersson, 1984; Schoen, 1970). This transformation, which is a transformation of bending without stretching relating two surfaces with the same Gaussian curvature, cannot be made without changing the identifications in the fundamental region, *i.e.* without tearing the surfaces, and this is why the intermediate steps appear as self-intersecting surfaces.

The identifications of the fundamental region needed to obtain the  $F$  surface are such that  $P_{64i}^3 = I$ . The symmetry operations of the  $F$  surface are thus the elements of  $\Phi_3^N$  in which all elements  $P_{64i}^3$  and elements obtained by transforming  $P_{64i}^3$  by other ele-

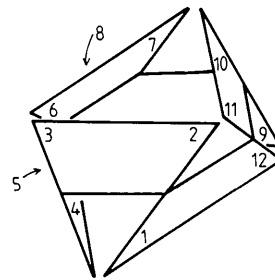


Fig. 15. The identification of the vertices of the dodecagonal cell leading to an element of surface topologically equivalent to that of the cell of the  $F$  surface. The polyhedron of Fig. 14 is obtained by reproducing this surface using a rhombohedral unit cell.

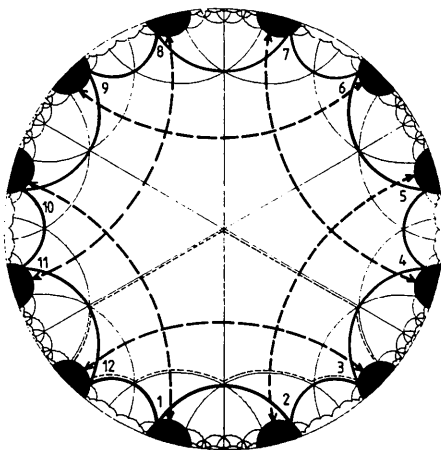


Fig. 13. In black are the parts of the hyperbolic plane which are to be cut out in order to permit the identifications leading to the  $P$  surface. The interrupted geodesic line, which represents a translation  $P_{66i}^2$ , forced to identity, crosses a crown of four squares of the  $\{4, 6\}$  tiling and is a cyclic line.

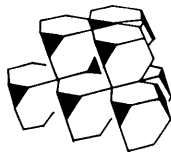


Fig. 14. An infinite polyhedron topologically equivalent to the  $F$  surface. It is a  $\{6, 6\}$  built from a truncated tetrahedron.

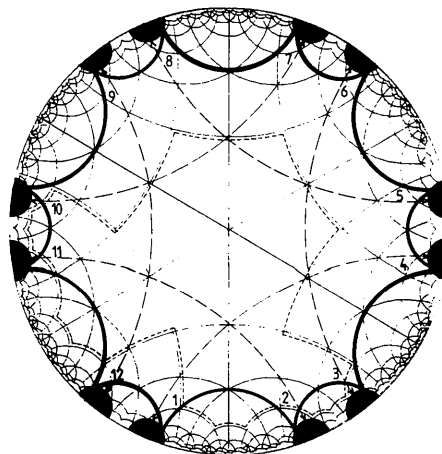


Fig. 16. In black are the parts of the hyperbolic plane which are to be cut out in order to permit the identifications leading to the  $F$  surface. The interrupted geodesic line, which represents a translation  $P_{64i}^3$ , forced to identity, crosses a crown of four hexagons of the  $\{6, 4\}$  tiling and is a cyclic line.

ments of  $\Phi_3^N$  are forced to identify. Here again generators  $t_i$  and  $\tau_i$  commute (see Appendix C) with the same consequences as in the case of the  $P$  surface. In Fig. 16 are shown parts of the  $\{6, 4\}$  tiling of the hyperbolic plane with the regions which are to be cut out in order to permit the identifications needed to obtain the  $F$  surface.

### III.3. Schoen's $G$ surface

This surface separates two oppositely congruent labyrinths of connectivity 3. It has no topological analogue made of infinite polyhedra with square or hexagonal flat faces but one might be built with the skew face drawn in Fig. 17. The fundamental region of the surface enclosed in the unit cell of the polyhedron is the dodecagonal one shown in Fig. 18. In this case the identifications are of a totally different type from those met in the cases of the  $P$  and  $F$  surfaces. The vertices are no longer identified in six sets of two but two sets of vertices are identified together and

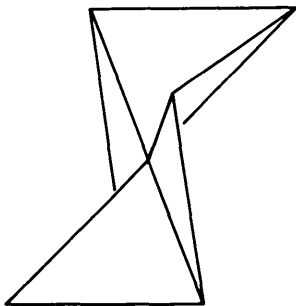


Fig. 17. The element of surface with flat faces supported by the Petrie polygon of the cube. It can be used to build a topological equivalent of the  $G$  surface by packing on a cubic lattice.

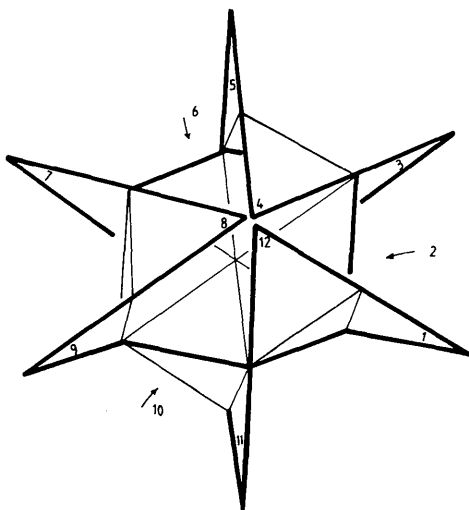


Fig. 18. The identification of the vertices of the dodecagonal cell leading to an element of surface topologically equivalent to that of the cell of the  $G$  surface.

the remaining six are left alone. The operations leading to this new type of identifications are  $P_{64i}^3 t_{i+1}^{-1} = I$  and  $P_{64i+3}^3 t_{i+1} = I$ , with  $i = 1, 2, 3$ . It is interesting at this stage to consider again the identification process used to make a cylinder from a Euclidean plane with a  $\{4, 4\}$  tiling. A cylinder can be obtained with an identification rule  $a_1^n = I$  and also with a more complex one  $a_1^n + a_2 = I$ . In the first case a lattice of circles and straight lines is drawn on the cylinder, whereas in the second case the lattice is drawn with helices. This second type of identification in the hyperbolic plane leads to the  $G$  surface. Here again  $t_i$  and  $\tau_i$  commute, but only  $\tau_i$  forms a basis for the Euclidean translation group in  $R_3$  (see Appendix C). For instance  $t_1 = \tau_1 \tau_3^{-1}$  and  $t_1 t_2 t_3 = I$ , so that the  $t_i$  are coplanar in this case. In Fig. 19 are shown parts of the  $\{6, 4\}$  tiling of the hyperbolic plane with the regions which are to be cut out in order to permit the identifications needed to obtain the  $G$  surface.

### IV. Concluding remarks

We recently analysed liquid crystalline structures formed by amphiphilic molecules as periodic systems of frustrated fluid films and showed that, in the particular case of 'bicontinuous' cubic phases, the frustration could be solved if the film was supported by the hyperbolic plane admitting a  $\{6, 4\}$  tiling. However, as a hyperbolic plane cannot be embedded in the Euclidean space  $R_3$ , it appeared that the film of the actual structure must indeed be supported by particular surfaces derived from the hyperbolic plane: the infinite periodic minimal surfaces of IPMS (Charvolin & Sadoc, 1987). At that time the exact mode of derivation was not clearly understood. We have tried to make precise the relationships existing

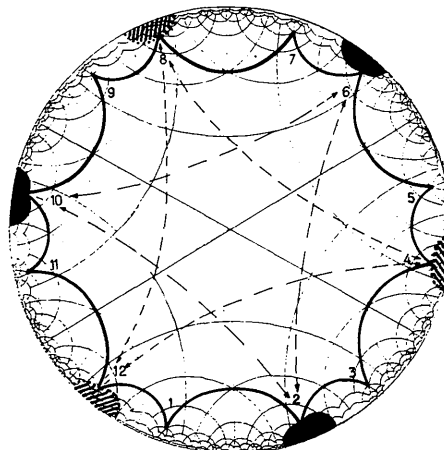


Fig. 19. In black and hatching are the parts of the hyperbolic plane which are to be cut out in order to permit the identifications leading to the  $G$  surface. In this case there is no cycle crossing elements of a regular tiling but helical lines.



between the hyperbolic plane and the IPMS in the present paper.

For this we considered the intrinsic geometry of this particular hyperbolic plane and analysed its symmetry groups, focusing our interest onto translation subgroups and fundamental regions. The periodic reproduction of the fundamental region by a translation subgroup covers the whole hyperbolic plane without overlap. Another representation of the periodic behaviour is that obtained by identifying the sides of the fundamental region two by two, so that all its vertices are gathered in one point, in order to build a toroidal surface. These two extreme representations are embedded in complex spaces. It is also possible to restrict attention to a small number of well chosen identifications and we show that, in some particular cases, the surfaces obtained are the IPMS embedded in  $R_3$ . These surfaces are obtained when some combinations of translations associated with the Petrie polygons of the tilings of the hyperbolic plane, as well as their combinations with elementary translations of the subgroup, are forced to identity. This imposes some 'surgery' in the hyperbolic plane, as some parts of it have to be cut out in order to permit the identifications, and implies also that the IPMS cannot keep a constant Gaussian curvature; it is only its averaged value which corresponds to that of the initial hyperbolic plane. These distortions are to be related to the fact that the whole hyperbolic plane cannot be embedded in  $R_3$  and the following simple argument can be used to illustrate this point. The number of points reproduced by elements of the symmetry group is infinite in all cases but we can look at the way it increases within a disk of increasing radius. In the hyperbolic plane this variation is exponential but follows a power law in  $R_3$ . Thus the hyperbolic plane is too 'large' to be put in  $R_3$  without the cutting out of some parts of its surface.

In this paper we considered a limited number of intermediate periodic representations only, three surfaces of genus 3 and cubic symmetry. Their exact number is certainly much larger, and may be infinite. In particular, surfaces of higher genus with larger fundamental regions should be considered. Another unsolved question is that of the condition ensuring that the surfaces built in that way are not self-intersecting surfaces. The solution probably requires a study of the properties of the commutators of the translation subgroup. While we have shown that these commutators become the identity when some translations are forced to identity to obtain the particular IPMS, we do not know the general condition for this. An important open question is also that of the relation between our transformation of one IPMS into another, by changing the identifications in the hyperbolic plane, and the well known Bonnet transformation relating surfaces of constant Gaussian curvature,

which should be the analytical counterpart of the first. In this problem concerning the transformation of IPMS without self-intersection, the first suggests that the second cannot be visualized continuously, without crossing surfaces with self-intersections.

Finally, we want to emphasize the interest of the crystallography of the hyperbolic plane whose application should not be limited to liquid crystalline structures but extended to the more general field of the physics of films and surfaces.

Fruitful discussions with E. Dubois-Violette and B. Pansu (Physique des Solides, Orsay), R. Mosseri (CNRS, Meudon) and P. Pansu (Ecole Polytechnique, Palaiseau) are gratefully acknowledged.

## APPENDIX A

### Demonstration that $t_i$ and $\tau_i$ are elements of [6, 4] and [6, 6]

With the operations defined in Fig. 9 the translation  $t_3 = B_3A_3$ .  $A_3$  and  $B_3$  are elements of [6, 4]; this proves that  $t_3$  and also  $t_i$  are elements of [6, 4].

$\tau_1 = B_3A_2B_2A_3$  if we write the translation as the product of two  $\pi$  rotations  $B_2A_3$  and  $B_3A_2$ . This expression for  $\tau_i$  proves that the  $\tau_i$  are elements of [6, 4].

Consider now other mirrors defined by edges of the central hexagon of the {6, 6} tessellation (and called  $a_1, a_2, a_3$  and  $b_1, b_2, b_3$ ; the centre of the edge which defines  $a_1$  is the common point of  $B_2$  and  $A_3$ ). Consider also mirrors which are symmetry mirrors of the central hexagon:  $M_1, M_2, M_3$  are such mirrors but there are three others called  $m_1, m_2, m_3$ . All the mirrors we have considered are elements of [6, 6].

We could write  $\tau_1 = b_1a_1$  and  $t_3 = m_3M_3(a_2M_3)^3$ .  $t_3$  is written as the product of two  $\pi$  rotations, because  $a_3M_3$  is a  $\pi/3$  rotation. These expressions prove that  $\tau_i$  and  $t_i$  are elements of [6, 6]. So  $\Phi_3^N$  is a subgroup of [6, 6] which is a subgroup of [6, 4], because  $t_i$  and  $\tau_i$  are generators of  $\Phi_3^N$ .

## APPENDIX B

### Networks for $P, F$ and $G$ surfaces

Figs. 20, 21 and 22 represent the primitive cells of the three IPMS, with one of the two networks in each

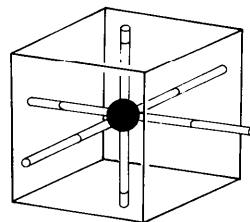


Fig. 20. Unit cell for the  $P$  surface. Only one labyrinth is shown. It is also the primitive cell of the simple cubic lattice.

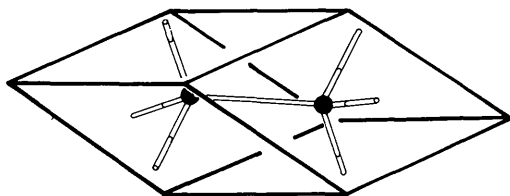


Fig. 21. Unit cell for the *F* surface. Only one labyrinth is shown. It is also the primitive cell of the face-centred-cubic lattice.

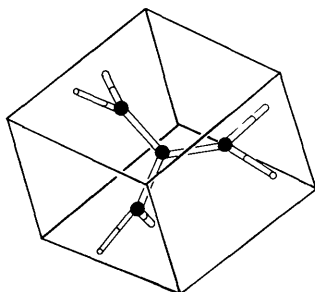


Fig. 22. Unit cell for the *G* surface. Only one labyrinth is shown. It is also the primitive cell of the body-centred-cubic lattice.

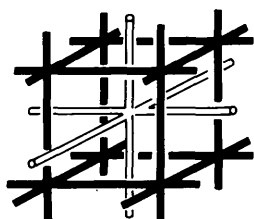


Fig. 23. The labyrinths of the *P* surface.

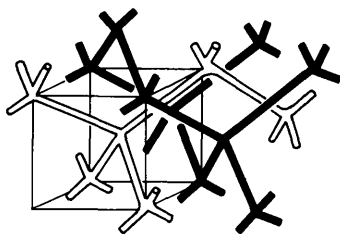


Fig. 24. The labyrinths of the *F* surface.

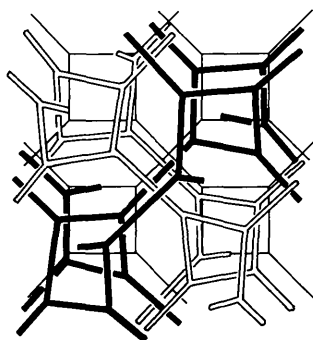


Fig. 25. The labyrinths of the *G* surface.

cell which is used to define the IPMS. Rods of these networks are orthogonal to faces of cells. In the *P* and *F* surface cases rods pierce faces at their centres; in the *G* surface they pierce the faces on the long diagonal in the ratio 3:8.

It is worth noting that it is possible to go from one network to another by a simple topological transformation. The connectivity of the node, which is 6 in the *P*-surface case, is 4 in the *F*-surface case but with two nodes in the cell, and decreases to 3 with three nodes in the cell from the *G* surface. This transformation is close to the  $T_1$  transformation introduced by Weaire & Rivier (1984).

Surfaces with the topology of the three IPMS are obtained by inflating rods. Then it is clear that they all have the same topology (Figs. 23-25).

### APPENDIX C

#### Calculation of some commutators

We give some examples of the method used to calculate commutators when some translations are identified to obtain the three IPMS.

For the *P* surface we impose  $(B_2B_1)^2 = I$  and similar relations with other  $B_i$  and  $A_i$ . Consequently  $B_iB_j$  and  $A_iA_j$  commute;  $B_iA_j$  also commutes because it is a  $\pi$  rotation.

$t_2^{-1}t_1^{-1}t_2t_1 = B_2A_2B_1A_1A_2B_2A_1B_1$  with the commutation rules leads to the commutation of  $t$  operations. With a similar calculation it can be shown that  $[\tau_i, \tau_j] = I$  and  $[t_i, \tau_i] = I$ .

For the *F* surface identification rules are of the type  $(M_3A_3M_1B_1)^3 = I$ ; we know that  $M_iA_i$  commutes and that  $M_3M_1 = M_1M_2 = M_2M_3$  are  $2\pi/3$  rotations. This leads to the identification rule  $A_1A_3A_2B_1B_3B_2 = I$ . With this form it can be shown that  $t$  and  $\tau$  operations commute.

For the *G* surface identification rules are of the type  $B_1A_1(M_1A_1M_2B_2)^2 = B_1B_3A_2A_3B_1B_2$ . With this expression and similar ones  $t_2^{-1}t_1^{-1}t_2t_1 = I$ . It can be shown also that commutators  $[\tau_i, \tau_j]$  and  $[t_i, \tau_j]$  are the identity.

With commutation relations the six identifications lead to  $t_i = \tau_1\tau_3^{-1}$ , and others by cyclic permutations. The three  $\tau_i$  form a basis, but the  $t_i$  do not because there is a relation  $t_1t_2t_3 = I$ .

#### References

- BALZAZS, N. L. & VOROS, A. (1986). *Phys. Rev.* **143**, 109.
- CHARVOLIN, J. & SADOE, J.-F. (1987). *J. Phys. (Paris)*, **48**, 1559-1569.
- COXETER, H. S. M. (1961). *Introduction to Geometry*. New York: John Wiley.
- COXETER, H. S. M. (1968). *Twelve Essays in Geometry*. Illinois: Carbondale.
- COXETER, H. S. M. & MOSER, W. O. J. (1957). *Generators and Relations for Discrete Groups*. Berlin: Springer.
- EKWALL, P. (1975). *Advances in Liquid Crystals*, edited by G. H. BROWN, Vol. 1, p. 1. New York: Academic Press.

- HILBERT, D. & COHN-VOSSEN, S. (1983). *Geometry and the Imagination*. New York: Chelsea.
- HYDE, S. T. & ANDERSSON, S. (1984). *Z. Kristallogr.* **168**, 213-221; 221-254.
- LUZZATI, V. (1968). *Biological Membranes*, edited by D. CHAPMAN, Vol. 1, p. 71. New York: Academic Press.
- MACKAY, A. L. (1985). *Nature (London)*, **314**, 604-606.
- MACKAY, A. L. & KLINOWSKI, J. (1986). *Comput. Math. Appl.* **12B**, 803-824.
- MAGNUS, W. (1974). *Non-Euclidean Tessellations and their Groups*. New York: Academic Press.
- SADOC, J.-F. & CHARVOLIN, J. (1986). *J. Phys. (Paris)*, **47**, 683-691.
- SCHOEN, A. H. (1970). *NASA Tech. Note No. D-5541*.
- SCHWARZ, H. A. (1890). *Gesammelte Mathematische Abhandlungen*. Bd 1, Berlin: Springer.
- SCRIVEN, L. E. (1976). *Nature (London)*, **263**, 123-125.
- SCRIVEN, L. E. (1977). *Micellization, Solubilization and Microemulsions*, edited by K. L. MITTAL, p. 877. New York: Plenum.
- WEAIRE, D. & RIVIER, N. (1984). *Contemp. Phys.* **25**, 59-99.
- WELLS, A. F. (1977). *Three-Dimensional Nets and Polyhedra*. New York: John Wiley.

*Acta Cryst.* (1989). **A45**, 20-25

## Crystal Elasticity and Inner Strain: a Computational Model

BY MICHELE CATTI

*Dipartimento di Chimica Fisica ed Elettrochimica, Università di Milano, via Golgi 19, 20133 Milano, Italy*

(Received 9 March 1988; accepted 11 July 1988)

### Abstract

The internal strain induced in a crystal structure by lattice deformation was considered. A suitable rotationally invariant representation was introduced and the corresponding contribution to the elastic constants was calculated. The method is based on the use of crystallographic rather than Cartesian atomic coordinates as variables of energy derivatives, with full exploitation of space-group symmetry and no constraint on the lattice geometry. A two-body Born interatomic potential was assumed, for both ionic and molecular crystals; energy derivatives of electrostatic lattice sums were calculated with the Ewald series. Molecular groups are treated within a rigid-body scheme based on Eulerian angles and translations as inner strain variables. Results of computations of  $\text{Mg}_2\text{SiO}_4$  (forsterite) are reported, and the importance of optimizing the potential parameters against experimental data is discussed.

### Introduction

Static models of crystals account for the response of the atomic structure to physical agents independent of temperature, such as mechanical stress and electric field. Being simpler than dynamic models, they provide an easier linkage between crystal properties and interatomic or intermolecular forces, by which the latter can be investigated. The property considered here is elasticity, following previous work (Catti, 1985) where the method of crystal static deformation to calculate elastic constants was outlined.

It is well known that when a crystal is stressed elastically, the induced deformation preserves the

translational symmetry and can be considered the superposition of a pure lattice (external) strain and of an internal strain (Born & Huang, 1954). The former keeps the atomic fractional coordinates constant, changing just the unit-cell geometry, while the latter does the opposite. In the previous paper the contribution of external strain to crystal elasticity was considered explicitly, whereas here attention is focused onto inner strain. This is actually a relaxation of the crystal structure responding to a forced lattice change; by taking it into account, not only are more reliable values of elastic constants calculated, but also the structure changes caused by an applied anisotropic stress can be predicted.

Recently, the subject of internal strain in crystal structures has drawn considerable attention. A general thermodynamic theory was developed, where inner strain is considered as an independent physical variable on the same footing as macroscopic thermodynamic quantities (Barron, Gibbons & Munn, 1971). Besides, a number of experiments on uniaxially stressed crystals have produced energy-level shifts related to atomic displacements, which can be detected through the study of Jahn-Teller effect, spin-lattice coupling in electron paramagnetic resonance (EPR), stress-induced linear dichroism and other methods (Cousins, 1981; Devine, 1983). The most direct experimental technique to probe internal deformations in crystals relies of course on the strain dependence of the intensity of elastic scattering of X-rays or neutrons (Segmüller, 1964). Computational methods are particularly valuable in this respect, owing to the difficulty of experiments on anisotropically stressed crystals and to the need of interpretation of results when these are available.